

Article

Parametric Optimisation of an ORC in a Wood Chipboard Production Facility to Recover Waste Heat Produced from the Drying and Steam Production Process

Yıldız Koç 

Department of Mechanical Engineering, Faculty of Engineering and Natural Sciences, Iskenderun Technical University, Hatay 31200, Turkey; yildiz.koc@iste.edu.tr; Tel.: +90-(538)-526-7033

Received: 14 August 2019; Accepted: 23 September 2019; Published: 25 September 2019



Abstract: The wastes in wood industries (waste chips) are commonly used as fuel for burners to produce steam and to use the remaining heat in the drying process. However, in spite of that, there is a considerable amount of heat evaluated from the burn of waste chips still released to the atmosphere without use. Therefore, in the present study, a cogeneration cycle design by used of ORC was designed and parametrically optimised for six organic working fluids (acetone, ethanol, R11, RE245fa2, R365mfc and R601a). During the ORC optimisation, the ORC turbine inlet temperature was changed from the saturated steam temperature of the fluid to the maximum temperature of the fluid. The ORC turbine inlet pressure was increased from 7.5 bar to the critical pressure of the fluid. As a result of the study, the maximum net power, net thermal efficiency and exergy efficiency of the ORC were found as 453.91 kW, 30.01% and 67.56% at 340 °C and 62.5 bar from the ORC with ethanol. This means that almost 30% of the waste heat could be recovered by use of the ORC with ethanol. By using the designed cogeneration system, it was calculated that the thermal efficiency of the system can be increased up to 74.01%.

Keywords: organic Rankine cycle (ORC); working fluids; wood chipboard; parametric optimization; exhaust gas; exergy

1. Introduction

Industrial sectors are giving great importance to plant optimisation and production optimization to meet the growing demand for products. However, although these sectors are sufficient to make the necessary improvements to meet the demand, the most important problems that almost all industrial production facilities cannot overcome are wastes [1,2]. In spite of all progress in industrial production technologies, nearly 6% of materials in iron and steel industry, 15% of materials in mining industry and 10% of materials in the food industry are still thrown to the environment as solid waste. [3–9]. Solid waste rates for the wood sector are also not negligible. In the wood industry, almost 80% of the raw material (wood) is used for production processes and the remaining proportion of the wood exits from the process as waste [10]. There are many additional sectors that use solid wastes of the wood industry as raw material. By these additional production processes, between 40% and 85% of the wastes can be recovered [11]. However, in spite of all efforts, there is still unusable solid wastes in the wood industry, which account for nearly 10% of the total wood input [10,11].

Although it is not possible to use this solid waste as a raw material in another process, it is possible to benefit from its thermal capacity. In wood-based production plants, steam and drying processes are essential and need high energy [12]. Therefore, there are many studies that analyse the use of the thermal capacity of unusable solid wood wastes [13–15]. Nunes et al. analysed the utilisation of the

woodchips as fuel in steam boiler [16]. Nunes et al. studied the economic and environmental benefits of the use of thermal energy of solid wood wastes. As a result of the study, by using wood chips, 27% of reduction in energy cost was calculated [17]. Barrier and Ghaffariyan evaluated the artificial wood drying process. After a detailed analysis, it was clearly seen that 17% of the total energy consumption was used for the drying process. They also mentioned that this energy need could be met by burning of wood wastes rather than natural gas [18]. Although the use of thermal energy of waste wood is an important recovery method, it is clear that it should be improved in terms of energy efficiency. Because a considerable proportion of the heat produced from the burning of wood wastes releases to the environment as waste by exhaust gas, many additional systems could be integrated into the waste wood combustion units for the recovery of this exhaust gas waste heat. Kalina cycles, organic Rankine cycles, recuperators and economisers are a couple of these waste heat recovery systems. Organic Rankine cycles are one of the best methods for the recovery of low and medium temperature heat sources [19–21]. Low cost, simple system configuration and high energy efficiency for use in low temperature heat sources are other important advantages of organic Rankine cycles [22–24].

There are many studies in the literature that have used organic Rankine cycles (ORC) to recover waste heat. Noussan et al. simulated a biomass fired CHP system and heat storage system. In the system, the heat used in ORC to produce power and the remaining proportion of the heat was stored to use in the distinct heating system [25]. Uris et al. assessed the feasibility of an ORC integrated cogeneration plant using biomass as fuel. In the designed system, the heat releasing from the burning of the biomass was used in ORC to produce electricity. After ORC, the remaining heat of the exhaust gas was sent to distinct cooling and heating system [26]. Safari and Dincer analysed novel biomass fired multigeneration system, which produces electricity, hot water, fresh water and hydrogen. As a result of the study, the amount of electricity, hot water, fresh water and hydrogen produced were calculated as 1102 kW, 1.82 kg/s, 0.94 kg/s and 0.347 kg/s, respectively [27]. Ghasemi et al. designed a multigeneration to produce heat, power, fresh water and to liquefy natural gas. After detailed calculations, 16.11 kW electricity, 28.94 kW heat, 8.8 kg/s fresh water and 0.02 m³/h liquefied natural gas production were seen as possible for a small scale multigeneration system [28]. Khanmohammadi and Atashkari modelled and optimised a polygeneration system that uses biomass as heat sources. As a result of the calculations, the exergy efficiency of the ORC and polygeneration system was found as nearly 27.3% and 27.9%, respectively [29]. Yağlı et al. integrated an ORC to a combined heat and power engine to recover waste heat of the exhaust gas. As a result of detailed calculations, the power production rate, thermal efficiency and exergy efficiency of the ORC were found as 81.52 kW, 15.93% and 27.76%, respectively [30].

In addition to the feasibility analysis of the integrating ORC to the waste heat source, it is also essential to parametrically optimise the ORC by considering different working fluids, turbine inlet pressure and turbine inlet temperature. There are many studies that parametrically optimised the ORC to obtain the best performing ORC parameters. Desideri et al. experimentally analysed an 11 kW ORC for the cases of using SES36 and R245fa as working fluid. As a result of the study, ORC reached a maximum thermal efficiency of 9% and 7.8% for the use of SES36 and R245fa, respectively [31]. Dicks et al. experimentally compared three approximations (constant-efficiency method, a polynomial-based method and a semi-empirical method) in order to obtain the best simulation method for ORC. As a result, the semi-empirical method presented the most reliable and precise results [32]. Peris et al. experimentally characterised the performance of an ORC to recover low grade waste heat in cement industry. After detailed experimental analysis, the maximum gross electrical efficiency of the ORC was found as 12.32% [33]. Yang et al. experimentally investigated 3 kW ORC for different operating parameters to recover low-grade waste heat. The experiment results showed that the maximum electrical power and thermal efficiency of the ORC was 1.89 kW and 5.92%, respectively [34]. Navarro-Esbri et al. experimentally studied and compared ORC using HFO-1336mzz-Z and HFC-245fa as a working fluid. During the experiments, the hot source temperature was varied from 140 °C to 160 °C, while the cold source temperature was varied from 25 °C to 40 °C. As a result of the study, the

maximum performance of the ORC was obtained from the case of using HFO-1336mzz-Z as a working fluid and at this state, the thermal efficiency was found to be 8.3% [35].

When all these studies are analysed together, the possibility of using ORC for recovering the exhaust gas of the waste wood fired burning is obviously seen. However, there are only limited studies that evaluate the usability of ORC for a chipboard production facility and almost none of them included the parametric optimisation of the ORC. Moreover, a considerable part of the studies used heat to produce hydrogen, fresh water and liquid natural gas rather than producing steam, which is essential for the chipboard production process. In addition to all these, there are only few studies which consider the needs of the facility throughout the production process.

In this study, a cogeneration system was designed for a wood chipboard production facility. The cogeneration system produces power by ORC and steam that is crucial for chipboard production. The unusable waste chips are used as fuel for the cogeneration system. After the design of the cogeneration system, the ORC system is parametrically optimised for six different working fluids (acetone, ethanol, R11, RE245fa2, R365mfc and R601a) for varying turbine inlet pressure (from 7.5 bar to the critical pressure of the fluid) and turbine inlet temperature (from saturated temperature of the fluid to the maximum temperature of the fluid). The optimisation of the ORC is made by use of EBSILON®Professional (EBSILON) software developed by Steag GmbH.

2. Cogeneration Cycle (CC)

The system analysed in the present study is designed to use in a wood chipboard production facility. In the facility, currently, waste wood chips coming from wood chipboard production is used as fuel to produce steam and to dry moist fibre. In the concept of this study, an ORC unit is integrated into a system to evaluate the cogeneration system and use excess heat of the exhaust gas. The schematic representation of the cogeneration system is given in Figure 1.

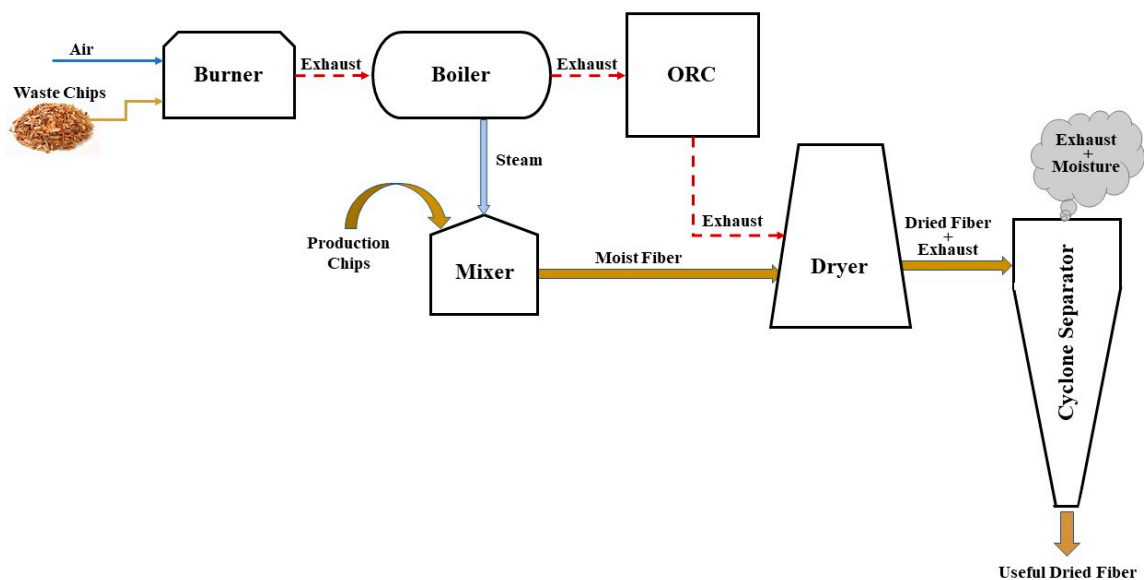


Figure 1. The schematic representation of the cogeneration system.

In the designed system, the exhaust gas evaluated by the burning of waste chips was cooled to the desired values by producing steam. The exhaust gas exits from the burner at around 600 °C temperature; this is so high for drying process due to the burning point of the wood fibres. Therefore, the exhaust gas sends to the boiler to produce the steam needed to soften production wood chips. Then, the exhaust gas is blown into an ORC unit at nearly 350 °C to produce electricity. After cooling down the exhaust gas to 160 °C, which is the desired temperature for the drying process, the gas is released into the dryer and mixes with moist fibre (with a relative humidity of 100%). Finally, the exhaust gas,

moisture and dried fibre (with a relative humidity of 11%) mixture separated from each other by using cyclone separator. The temperature and relative humidity values of each step were taken from the facility. However, each value varied slightly throughout the day. In order to have a better result and optimise ORC for various working fluid, the system parameters were taken as the average value of a day. The system parameters accepted constant for cogeneration system is given in Table 1.

Table 1. The additional design and parametric optimisation assumptions for the ORC.

Parameter	Value	Unit
Burned waste chip amount	967	kg/h
Moist fibre amount (relative humidity 100%)	2765.841	kg/h
Useful dried fibre amount (relative humidity 11%)	1681.106	kg/h
Exhaust gas mass flow	7.68	kg/s
Steam mass flow	0.815	kg/s
Burner exit temperature	600	°C
Boiler exit temperature	350	°C
ORC exit temperature	160	°C
Dryer exit temperature	60	°C

3. Organic Rankine Cycle (ORC)

3.1. Description of the ORC

The wood chips used to produce wood chipboard were raw materials sensitive to high temperature. Therefore, in order to minimise the adverse effect of high temperature on wood chips, the exhaust gas exiting from the boiler was cooled by the air to lower its temperature up to 160 °C. However, the heat released into the atmosphere had high heat content and could be used in ORC to recover. By considering all these, in the present study, an ORC is integrated into the system to improve overall system efficiency. The schematic representation and temperature-entropy change diagram of the ORC are shown in Figure 2.

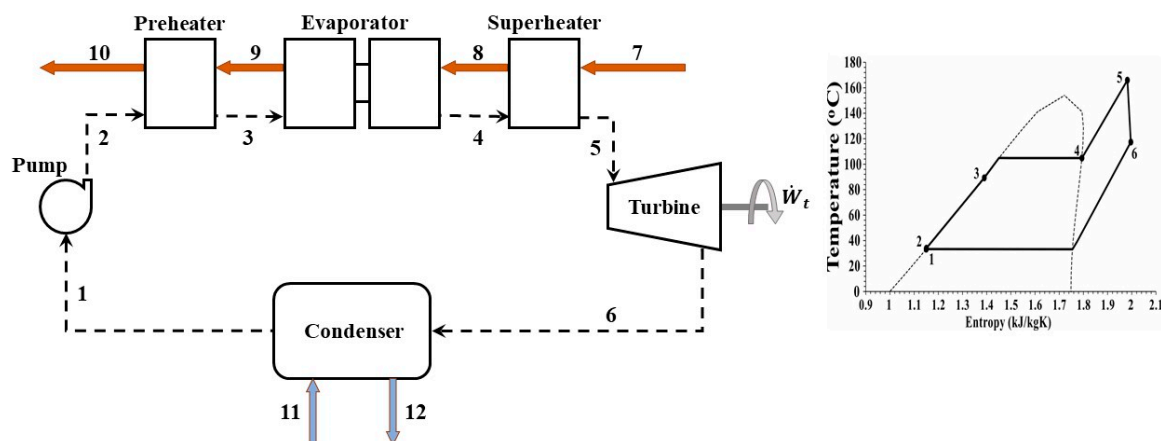


Figure 2. The schematic representation and temperature-entropy change diagram of the ORC.

The designed ORC has three components on the hot side (preheater, evaporator and superheater) to be able to recover high energy as much as possible. In the hot side of the ORC, the heat of the exhaust gas coming from the boiler is transferred to the pressurised working fluid. Then, the pressurised and hot working fluid, which is in the superheated vapour state, was expanded in the turbine to generate shaft power. After the expansion, the low-pressure working fluid goes into the condenser to cool down. Finally, the working fluid was released into the pump to increase its pressure to the desired levels. Throughout the study, the system is optimised for six different working fluids to evaluate the best performing ORC condition and increase overall cogeneration system efficiency. During the

parametric optimisation of the ORC, some system parameters were accepted as constant, which are given in Table 2.

Table 2. The accepted nominal working parameters for ORC.

Parameter	Value	Unit
Isentropic efficiency of the pump [36–39]	80	%
Isentropic efficiency of the turbine [30,40–42]	88	%
Cooling water inlet temperature	20	°C
Exhaust gas inlet temperature	350	°C
Exhaust gas outlet temperature	160	°C
Exhaust gas mass flow rate	7.68	kg/s

3.2. Working Fluids of the ORC

The ORC units are the most convenient system to recover the heat of low and medium temperature heat sources to electricity. However, in order to evaluate the best performing ORC, the selection of working fluids is essential [43,44]. There are many fluid selection criteria, such as thermodynamic properties, environmental effect and price [45,46]. There are two parameters to decide the effect of working fluids on the environment, which are Ozone Depletion Potential (ODP) and Global Warming Potential (GWP) [47,48]. One of the most important selection criteria is the type of working fluids. The working fluid divided into three sub-groups, which are dry, isentropic and wet. The type of a working fluid is specified by considering the slope of the saturated vapour line. If the slope of the saturated vapour line is negative, the fluid is called a dry fluid. When the slope is equal to zero, this type of fluid is named isentropic fluid. The positive slope fluids are called wet type fluids. In the concept of the study, six different working fluids were selected to parametrically optimise the ORC. The thermodynamic properties and types of the selected working fluid are shown in Table 3.

Table 3. The thermodynamic properties and types of the selected working fluid [43,49–56].

Name	T_{boil}^*	P_{cond}^{**}	T_{crt}	P_{crt}	T_{max}	ODP	GWP	Type
	°C	bar	°C	bar	°C	-	-	-
Acetone	56	0.38	234.90	46.00	276.00	n.a.	n.a.	wet
Ethanol	78.00	0.11	241.56	62.68	376.00	n.a.	n.a.	wet
R11	23.00	1.26	197.96	44.07	351.85	1	4600	isentropic
RE245fa2	28.89	1.04	171.73	34.33	226.85	0	812	dry
R365mfc	39.82	0.693	186.85	32.66	226.85	0	825	dry
R601a	27.40	1.09	187.20	33.78	226.00	0	~20	dry

* at 1 bar; ** at 30 °C

The selected working fluids have an ignorable or minor adverse effect on the environment when the ODP and GWP values considered together. However, when the flammability of these fluids is considered, the fluid had moderate and high flammability rates, just like most organic fluids. In literature, there are many studies that use flammable fluids [57,58]. However, the danger of these fluids is that the performance of the ORC with these fluids is generally found to be higher. Therefore, in order to reduce the adverse effect of these flammable and toxic fluids, many studies have been studied to find precautions and to eliminate the adverse effect of these fluids on the environment for the use of these fluids in the power cycles [59–61]. Further research suggests alternative precautions systems such as microelectronic systems (cooling of central processing units—CPU) to eliminate the flammability of these fluids [62].

In this study, two wet types, one isentropic type and three dry type working fluids were used in the ORC, to see the effect of fluid type together with the performance of working fluids. Some of the selected fluids are commonly used working fluids in the literature (RE245fa2, Ethanol and R11). However, the remaining fluids are rarely used working fluids in the literature. As a result of the study,

the performance of the commonly used and rarely used working fluids were compared to present the best performing working fluid for various turbine inlet temperature and turbine inlet pressure.

4. Mathematical Model

In the performance calculation of the ORC, basic equations of the first and second law of thermodynamics were used. The general mass, energy and exergy balance of the system can be written as [63–69]:

$$\sum \dot{m}_i = \sum \dot{m}_e, \quad (1)$$

$$\dot{Q} + \dot{W} = \sum \dot{m}_e h_e - \sum \dot{m}_i h_i, \quad (2)$$

$$\dot{E}_i = \dot{E}_e + \dot{E}_d, \quad (3)$$

where \dot{Q} , \dot{W} and \dot{E} represents heat, work and exergy flow, respectively. The exergy flow can be calculated by:

$$\dot{E} = \dot{m}\psi, \quad (4)$$

where the notation ψ is the specific exergy and can be found by:

$$\psi = (h - h_0) - T_0(s - s_0), \quad (5)$$

Exergy means beneficial work, thus, the work has 100% efficiency in terms of exergy. However, the heat has lower exergy efficiency than 100%. Thus, the exergy flow of the heat in the burner is determined by:

$$\dot{E}_{heat} = \dot{Q}_{fuel} \left(1 - \frac{T_0}{T_{sur}}\right), \quad (6)$$

where T_0 is the room temperature and T_{sur} is the temperature of the heat transferring surface. During the calculations, the average temperature is assumed as the room condition temperature. The heat transferring surface temperature is accepted as the average of the input and output temperatures of the equipment. The heat supplied to the system by the burner from the burning of the chips is calculated by [70]:

$$\dot{Q}_i = \dot{m}_{WC} LHV_{WC} \epsilon_{burner}, \quad (7)$$

where LHV_{WC} is the lower calorific value of the waste wood chips and this value is equal to almost 17,500 kJ/kg. The ϵ_{burner} is the effectiveness of the burner, which is recorded as 96% from the plant.

The overall energy and exergy efficiency of the system should be calculated in order to make a final decision on the suitability and usefulness of the power systems. For this reason, both the energy and exergy efficiencies were calculated for ORC and the cogeneration system. The energy efficiency of the simple gas turbine, ORC and cogeneration system are calculated by:

$$\eta_{ORC} = \frac{\dot{W}_{ORC,net}}{\dot{Q}_{evap}}, \quad (8)$$

$$\eta_{CC} = \frac{\dot{W}_{ORC,net} + \dot{Q}_{boiler} + \dot{Q}_{dryer}}{\dot{Q}_i}, \quad (9)$$

where $\dot{W}_{ORC,net}$ represents the net power production from ORC and \dot{Q}_{evap} represents the heat inlet to the ORC on the hot side. \dot{Q}_{boiler} and \dot{Q}_{dryer} means heat transferred in the boiler and dryer. The exergy efficiency of the simple gas turbine, ORC and cogeneration system are found by:

$$\epsilon_{ORC} = \frac{\dot{W}_{ORC,net}}{\dot{E}_{evap}}, \quad (10)$$

$$\varepsilon_{CC} = \frac{\dot{W}_{ORC,net} + \dot{E}_{boiler} + \dot{E}_{dryer}}{\dot{E}_i} \quad (11)$$

During the calculations, some assumptions were made, such as accepting the steady-state conditions and the negligible kinetic and potential energies. The room temperature was accepted as 18 °C.

5. Results and Discussion

5.1. Parametric Optimisation Results of the ORC

In the first step of the calculations, the heat of the exhaust gas exiting from the steam boiler is recovered by using ORC rather than cooling by the heat exchanger to lower the temperature up for the drying process. The ORC integrated to the system was parametrically optimised for varying turbine inlet temperature (from saturated temperature to the maximum temperature of the fluid) and for varying turbine inlet pressure (from 7.5 bar to the critical pressure of the working fluid). The turbine outlet pressure (condensing pressure) of the ORC was equal to the saturated steam pressure at a temperature of 30 °C, which is given in Table 3. Throughout the parametric optimisation analysis, six different fluids (acetone, ethanol, R11, RE245fa2, R365mfc and R601a) were used as working fluids. The mass flow rate of the organic working fluids for varying turbine inlet temperatures and turbine inlet pressures are given in Figure 3.

When the change in organic working fluid mass flow rate was analysed, a continuous decrease was seen with increasing turbine inlet temperature at constant turbine inlet pressure since the heat entering the ORC was constant. However, at a constant turbine inlet temperature, the working fluid mass flow rate increased with an increasing turbine inlet pressure. When the mass flow rate values were analysed by considering the working fluids, the highest mass flow rate was calculated for R11, which is an isentropic type fluid. The wet types of working fluids (acetone and ethanol) have the lowest mass flow rate when compared with the other type of working fluids. The maximum and minimum mass flow rate is calculated as 7.204 kg/s (at 198 °C and 44 bar) and 1.004 kg/s (at 340 °C and 7.5 bar) for R11 and ethanol, respectively. Since the heat entering the ORC is constant, the reason for the maximum fluid mass flow rate of the ORC with R11 is thought to be due to low specific heat and turbine inlet temperature. The amount of the mass flow rate is one of the parameters that affect the gross and net power production. The gross power production of the ORC is taken as a turbine shaft power and pump power consumptions are not considered while calculating the gross power. The gross power values calculated from the ORC turbine for varying turbine inlet temperatures and turbine inlet pressures are shown in Figure 4.

At constant turbine inlet pressure, gross power lines showed different changing trends depended on the fluid type. At constant turbine inlet pressure, the gross power values increased with an increasing turbine inlet temperature for wet and isentropic type working fluids (acetone, ethanol and R11). However, for dry type working fluids, two changing trends in the gross power values were observed. At constant turbine inlet pressure, the gross power production was decreased with increasing turbine inlet temperature up to high turbine inlet pressure levels. At high turbine inlet pressure levels, the gross power production of the ORC first increased up to a certain turbine inlet temperature, and then decreased with an increasing turbine inlet temperature. The minimum and maximum gross power production were calculated as 164.34 kW (at 225 °C and 7.5 bar) and 464.51 kW (at 340 °C and 62.5 bar) for the ORC with RE245fa2 and ethanol, respectively. In addition to gross power production, calculation of the net power production is also crucial to decide the performance of the ORC, because the power production of the ORC is one of the important factors to specify the available power. The net power of the ORC is calculated by subtracting the pump power consumption from the gross power. The net power evaluated from the ORC for varying turbine inlet temperatures and turbine inlet pressures is presented in Figure 5.

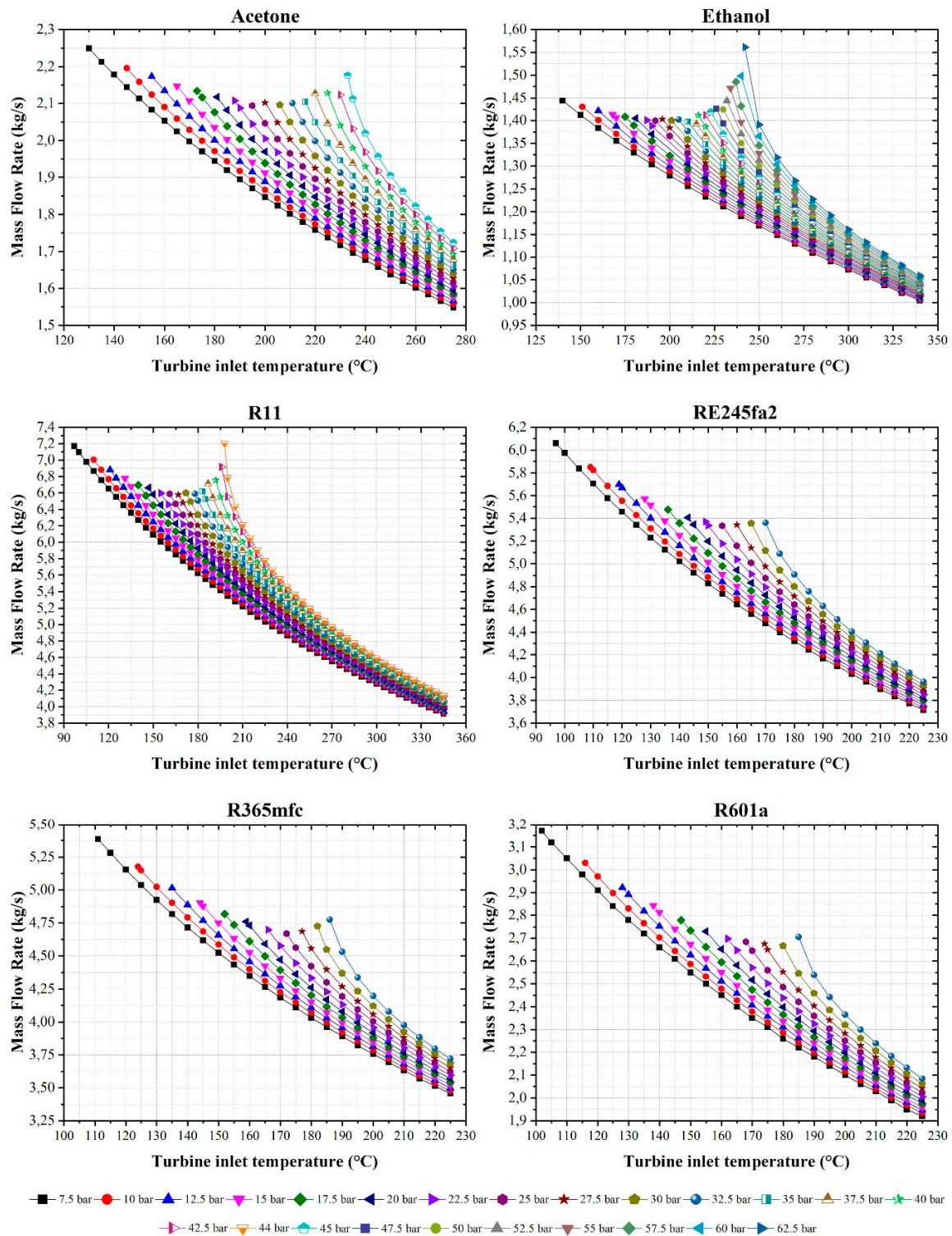


Figure 3. The mass flow rate of the organic working fluids for varying turbine inlet temperatures and turbine inlet pressures.

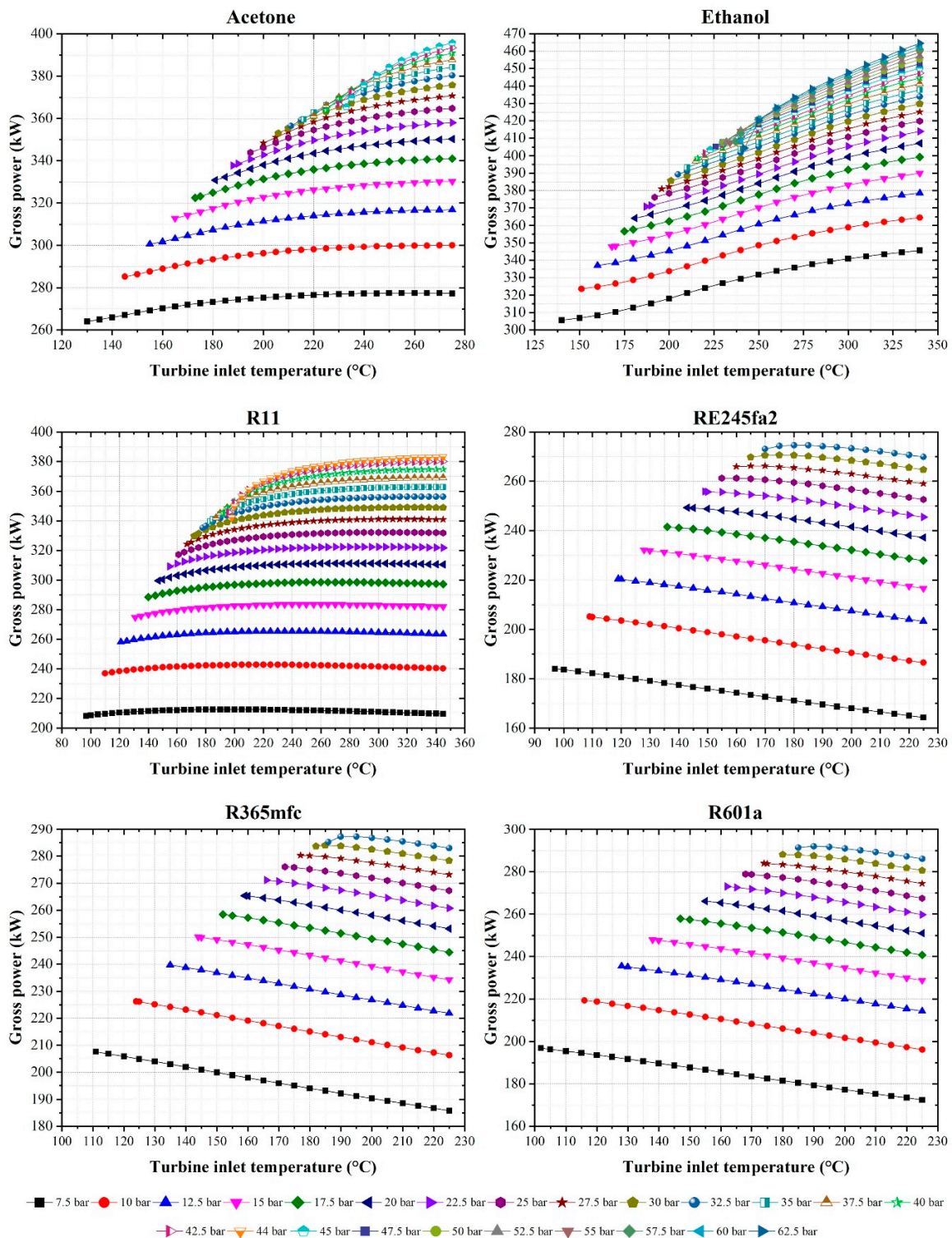


Figure 4. The gross power values calculated from the ORC turbine for varying turbine inlet temperatures and turbine inlet pressures.

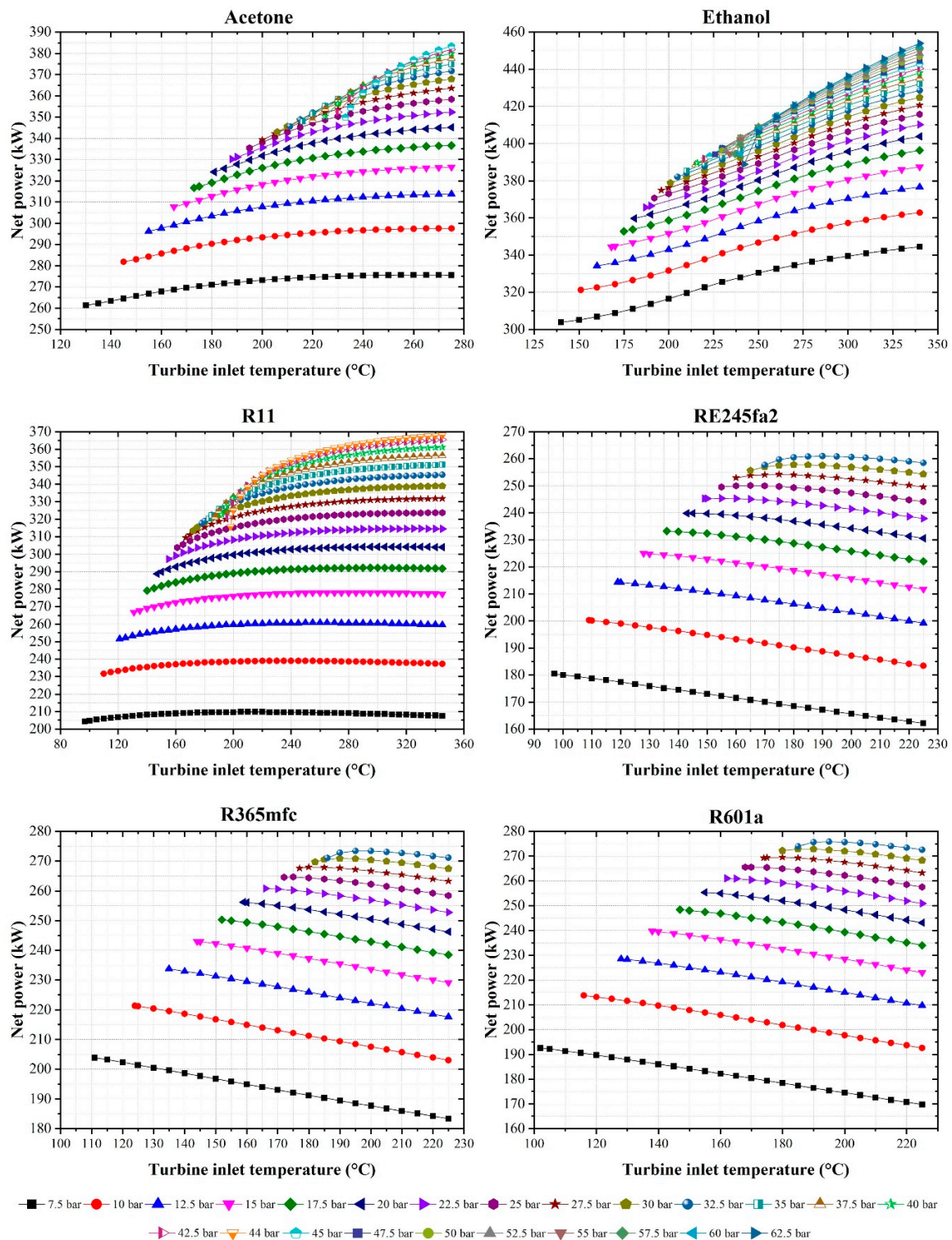


Figure 5. The net power evaluated from the ORC for varying turbine inlet temperatures and turbine inlet pressures.

The net power production of the ORC increased for all working fluids with an increasing turbine inlet pressure at a constant turbine inlet temperature. However, at constant turbine inlet pressure, just like the gross power production, the net power production also shows different changing trends dependent on the fluid type. The wet and isentropic types of working fluids have the same trend, while the dry type working fluids shows similar trends among themselves, but a different trend from

other types of working fluids. When the working fluids are sorted in terms of the net power produced, it can be sorted as ethanol, acetone, R11, R601a, R365mfc and RE245fa2 from highest to the lowest. The minimum and maximum net power production of the ORC was evaluated from RE245fa2 and ethanol as 162.12 kW at 225 °C—7.5 bar and 453.91 kW at 340 °C—62.5 bar, respectively. Another parameter considered throughout the parametric optimisation of the ORC is gross thermal efficiency, which was calculated by the ratio of gross power production with heat entering the ORC. The gross thermal efficiencies calculated from the ORC for varying turbine inlet temperatures and turbine inlet pressures are given in Figure 6.

The gross thermal efficiency of the ORC is an important parameter to have a vision on pump consumption. The change in gross thermal efficiencies for each working fluid shows the same tendency with gross power production. As a result of the calculations, the minimum gross thermal efficiencies were calculated at 7.5 bar turbine inlet pressure as 18.41% (at 130 °C), 20.21% (at 140 °C), 13.77% (at 97 °C), 11.46% (at 225 °C), 12.96% (at 225 °C) and 12.02% (at 225 °C) for acetone, ethanol, R11, R345fa2, R365mfc and R601a, respectively. Moreover, the maximum gross thermal efficiencies were calculated as 27.6% (at 275 °C—45 bar), 30.71% (at 340 °C—62.5 bar), 25.33% (at 345 °C—44 bar), 19.15% (at 180 °C—32.5 bar), 20.04% (at 190 °C—32.5 bar) and 20.37% (at 190 °C—32.5 bar) for acetone, ethanol, R11, R345fa2, R365mfc and R601a, respectively. Although the gross thermal efficiency is one of the important parameters for the ORC systems, it is essential to analyse net thermal efficiency of the ORC to have an exact decision on the pump power consumption rate and its effect. Therefore, the net thermal efficiency of the ORC is also calculated, the results of which are presented in Figure 7.

The net thermal efficiency of the system was found from the ratio of the net power production to the total heat input to the ORC. Since the pump power consumption was taken into consideration, the net thermal efficiency gave a perspective on the effects of these parameters on cycle performance. Therefore, the difference between the gross thermal efficiency and net thermal efficiency was directly related to ORC pump power consumption. As a result of the calculations, the minimum net thermal efficiencies were calculated at 7.5 bar turbine inlet pressure as 18.23% (at 130 °C), 20.1% (at 140 °C), 13.51% (at 97 °C), 11.31% (at 225 °C), 12.8% (at 225 °C) and 11.84% (at 225 °C) for acetone, ethanol, R11, R345fa2, R365mfc and R601a, respectively. Moreover, the maximum net thermal efficiencies are calculated as 26.73% (at 275 °C—45 bar), 30.01% (at 340 °C—62.5 bar), 24.33% (at 345 °C—44 bar), 18.2% (at 190 °C—32.5 bar), 19.07% (at 195 °C—32.5 bar) and 19.24% (at 195 °C—32.5 bar) for acetone, ethanol, R11, R345fa2, R365mfc and R601a, respectively. When compared with the gross thermal efficiency, the effect of the working fluid on the ORC is obviously seen, because the minimum net and gross thermal efficiencies of each working fluid were calculated at the same turbine inlet temperature and turbine pressure. However, the maximum net and gross thermal efficiencies of each working fluid were only found at the same turbine inlet temperature and turbine pressure for the wet and isentropic type working fluids. The maximum net and gross thermal efficiencies dry type working fluids were calculated at the same turbine inlet pressure but different turbine inlet temperature. This is thought to result from the mass flow rate and pump power consumption at high pressure levels. Loni et al. applied a thermodynamic based analysis to an ORC. In the study, ethanol and R601 were selected as working fluid as well as other some working fluids. As a result of the analysis, the thermal efficiency of the ethanol were found to be higher than R601 and the thermal efficiency of ORC with ethanol was found between 22% and 24% [71]. Dumont et al. applied technical and economic optimization procedures on an ORC. As a working fluid, they selected R134a, R245fa, Butane, n-Pentane, Ethanol, R1233zd(E) and R1234yf. As a result of detailed calculations, ORC with ethanol showed better performance than ORC with R245fa [72]. Another important parameter calculated for ORC is the exergy efficiency of the ORC. The exergy efficiency of the ORC considers useful work and heat. Therefore, exergy-based efficiency calculations give a more accurate and exact perspective on the performance of a cycle. The exergy efficiency calculated from the ORC for varying turbine inlet temperatures and turbine inlet pressures is shown in Figure 8.

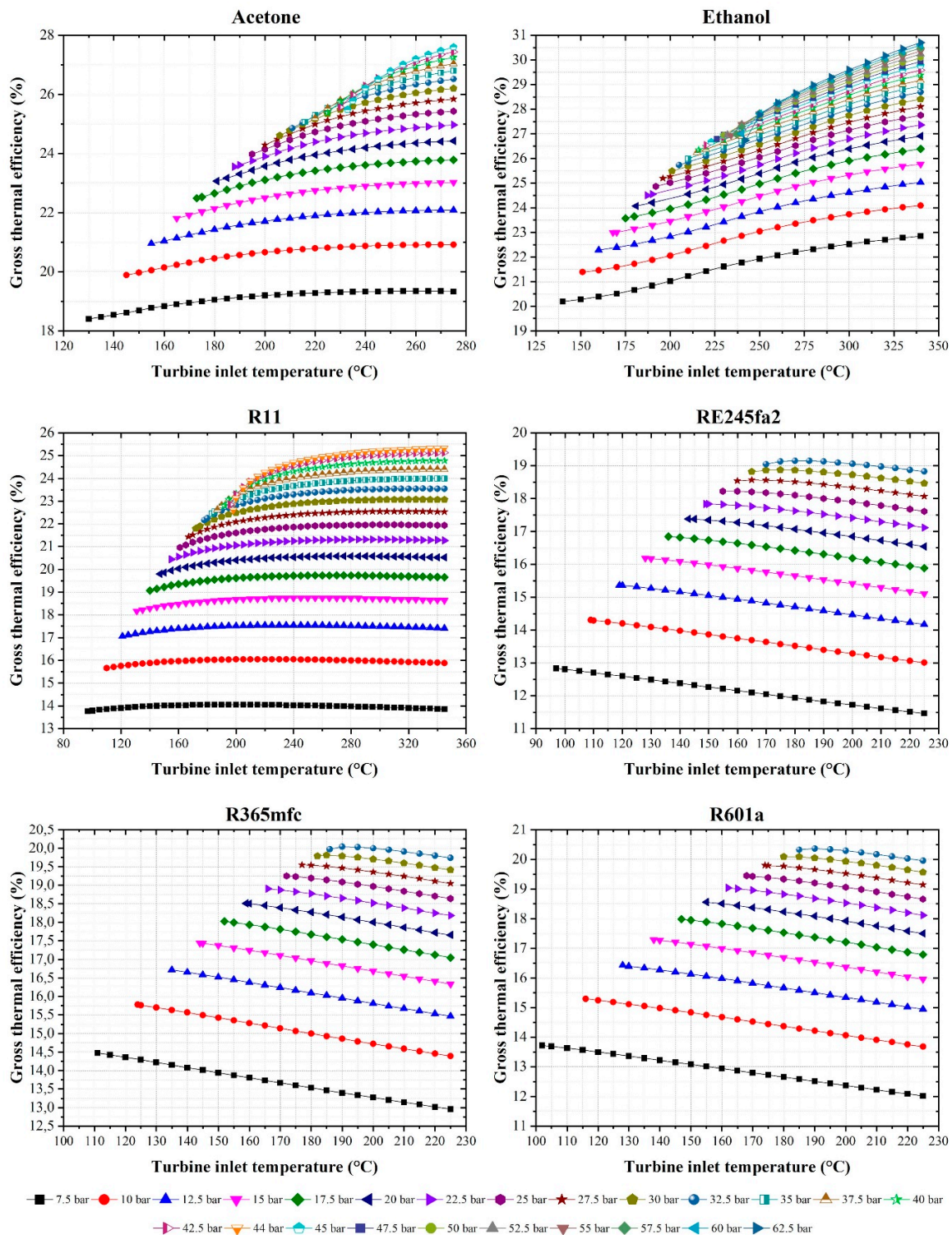


Figure 6. The gross thermal efficiency calculated from the ORC for varying turbine inlet temperatures and turbine inlet pressures.

The exergy efficiency of the ORC shows same changing tendency with gross and net power production. However, the maximum exergy efficiency was calculated at the same turbine inlet parameters of the net power production of the ORC rather than gross power production of the ORC. When the working fluids are sorted in term of the maximum evaluated exergy efficiencies, it can be sorted as ethanol (67.56%), acetone (60.2), R11 (54.77%), R601a (43.31%), R365mfc (42.93%) and RE245fa2 (40.97%), respectively. Loni et al. calculated the exergy efficiency of the ORC using ethanol

and R601 in their study. In the results of the study, the exergy based efficiency of the ORC with ethanol increased from 45% to 55%, which are considerably higher than the exergy efficiency of the ORC with R601 [71].

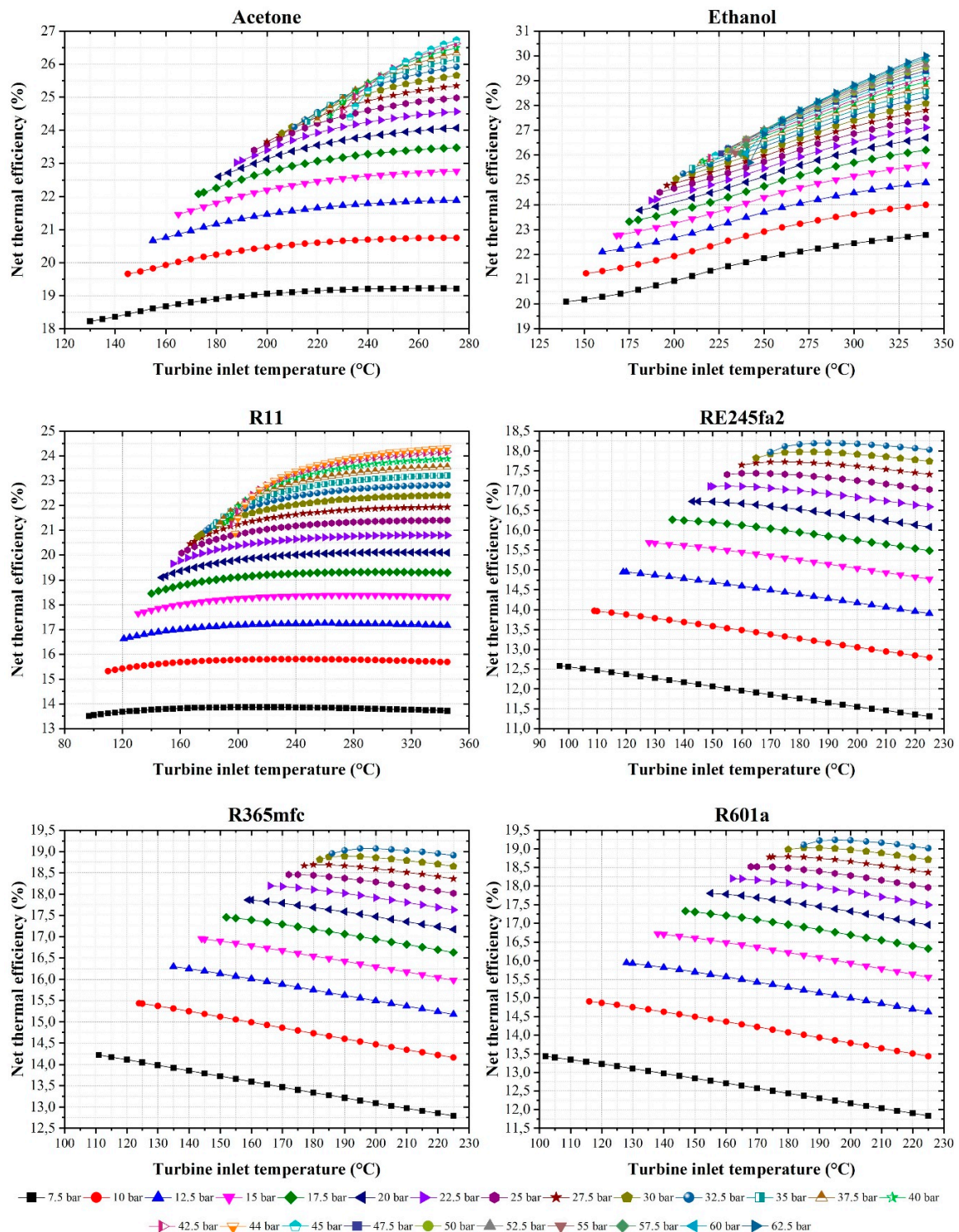


Figure 7. The net thermal efficiency calculated from the ORC for varying turbine inlet temperatures and turbine inlet pressures.

When all ORC parameters were considered together, it can be clearly seen that the ORC with ethanol had the best performance for all turbine inlet temperature and turbine inlet pressure levels.

The type of working fluid has an important role in the safety and life of the turbine. However, the most important factor for a power cycle is the evaluated net power. Therefore, although the dry and isentropic type of working fluids presents longer turbine life, the performance of these types of fluids are found considerable low in the study.

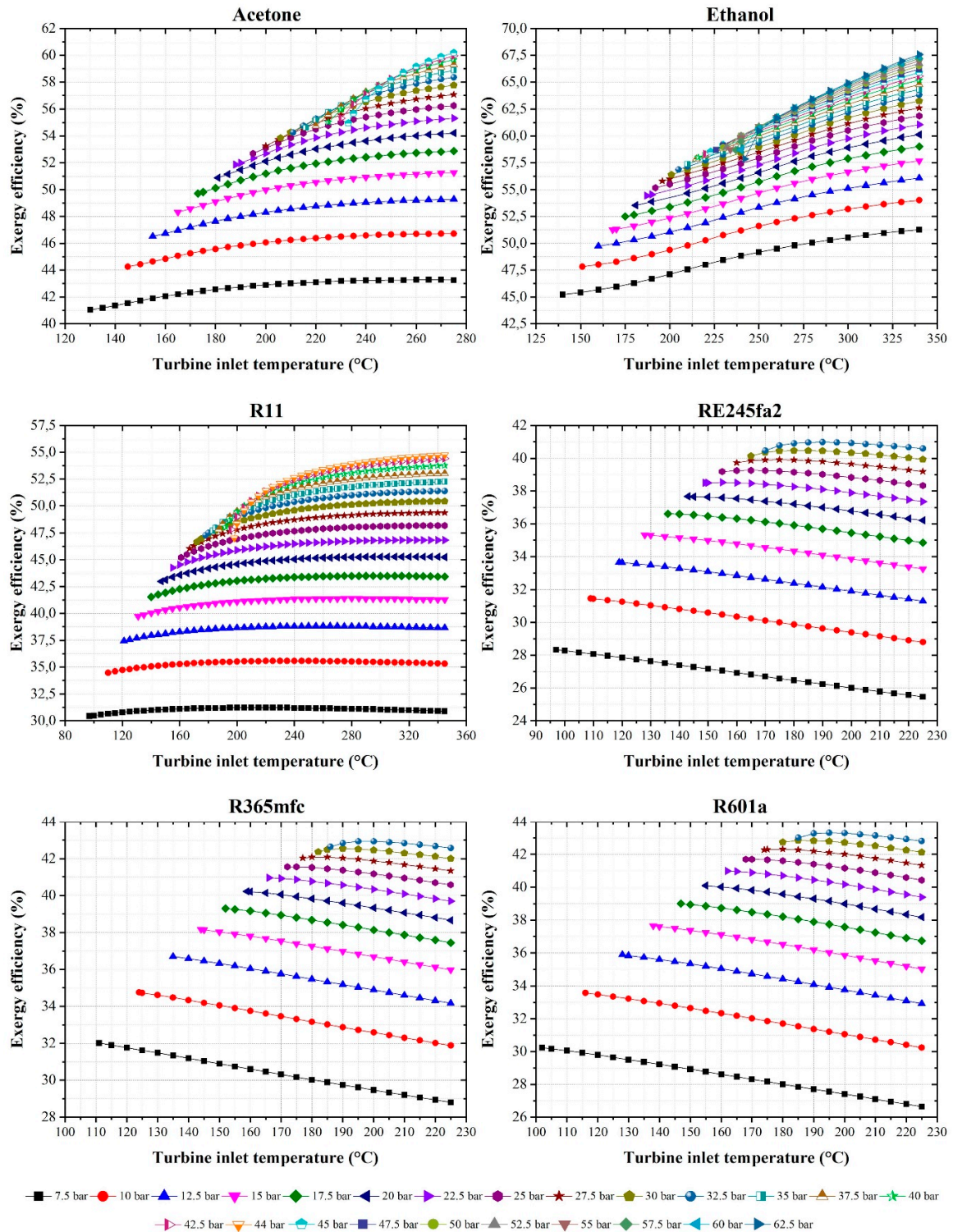


Figure 8. The exergy efficiency calculated from the ORC for varying turbine inlet temperatures and turbine inlet pressures.

5.2. Performance Parameters of the Cogeneration Cycle

After the parametric optimisation of the ORC, the performance of the overall cogeneration system is analysed by calculating the overall thermal and exergy efficiencies of the system. As a result of the calculations, the change in the thermal efficiency of the cogeneration cycle by considering the selected organic working fluids, ORC-turbine inlet temperature and ORC-turbine inlet pressure is shown in Figure 9.

In the current system, the exhaust gas is cooled in the heat exchanger to use in the fibre drying process. The released heat in the heat exchanger is thrown directly to the atmosphere without use. With the present study, an alternative cogeneration cycle is suggested by adding ORC to the system. After parametric optimisation and detailed calculations, almost 30% of the wasted heat is calculated as recoverable by use of ORC with ethanol. By using the designed cogeneration system, it was calculated that the thermal efficiency of the system can be increased up to 74.01%. When the parametric optimisation results of the ORC with selected fluids were considered together for varying ORC-turbine inlet temperature and pressure, the maximum cogeneration cycle efficiency was calculated as 74.01% (at 340 °C—62.5 bar) for ethanol, 72.51% (at 275 °C—45 bar) for acetone, 72.17% (at 345 °C—44 bar) for R11, 70.21% (at 195 °C—32.5 bar) for R601a, 70.15% (at 195 °C—32.5 bar) for R365mfc and 69.8% (at 190 °C—32.5 bar) for RE245fa2. In addition to the thermal efficiency of the cogeneration cycle, the exergy efficiency of the cogeneration cycle was also calculated in the scope of the present study. The change in exergy efficiency of the cogeneration cycle by considering the selected organic working fluids, ORC-turbine inlet temperature and ORC-turbine inlet pressure is given in Figure 10.

When the parametric optimisation results of the ORC with selected fluids were considered together for varying ORC-turbine inlet temperature and pressure, the maximum cogeneration cycle exergy efficiency was calculated as 82.24% (at 340 °C—62.5 bar) for ethanol, 79.33% (at 275 °C—45 bar) for acetone, 78.7% (at 345 °C—44 bar) for R11, 74.90% (at 195 °C—32.5 bar) for R601a, 74.79% (at 195 °C—32.5 bar) for R365mfc and 74.27% (at 190 °C—32.5 bar) for RE245fa2. When the exergy efficiency results of the ORC for varying turbine inlet pressure and turbine inlet temperature were considered together, the maximum exergy efficiency of the combined cycle was calculated as 82.24% for ethanol used ORC. This means that a considerable amount (82.24%) of the available energy entering the cogeneration cycle by burning of waste chips was used in the system. Integrating the ORC cycle to the present system will improve the overall performance of the system and reduce the adverse effect on the environment and global warming. In order to show the best performing ORC points and performance parameters obtained at these points, a summary table is prepared and presented in Table 4.

Table 4. The maximum performance obtained cycle parameters for each working fluid.

Name	$T_{ORC-tur,in}$	$P_{ORC-tur,in}$	\dot{m}_{ORC}	\dot{W}_{ORC}	η_{ORC}	ϵ_{ORC}	η_{CC}	ϵ_{CC}
	°C	bar	kg/s	kW	%	%	%	%
Acetone	275	45.0	1.72	383.32	26.73	60.18	72.50	79.30
Ethanol	340	62.5	1.06	453.91	30.01	67.56	74.01	82.24
R11	345	44.0	4.14	368.00	24.33	54.77	72.18	78.70
RE245fa2	190	32.5	4.63	260.96	18.20	41.00	69.90	74.28
R365mfc	195	32.5	4.34	273.40	19.10	42.93	70.16	74.80
R601a	195	32.5	2.44	275.86	19.24	43.31	70.21	74.90

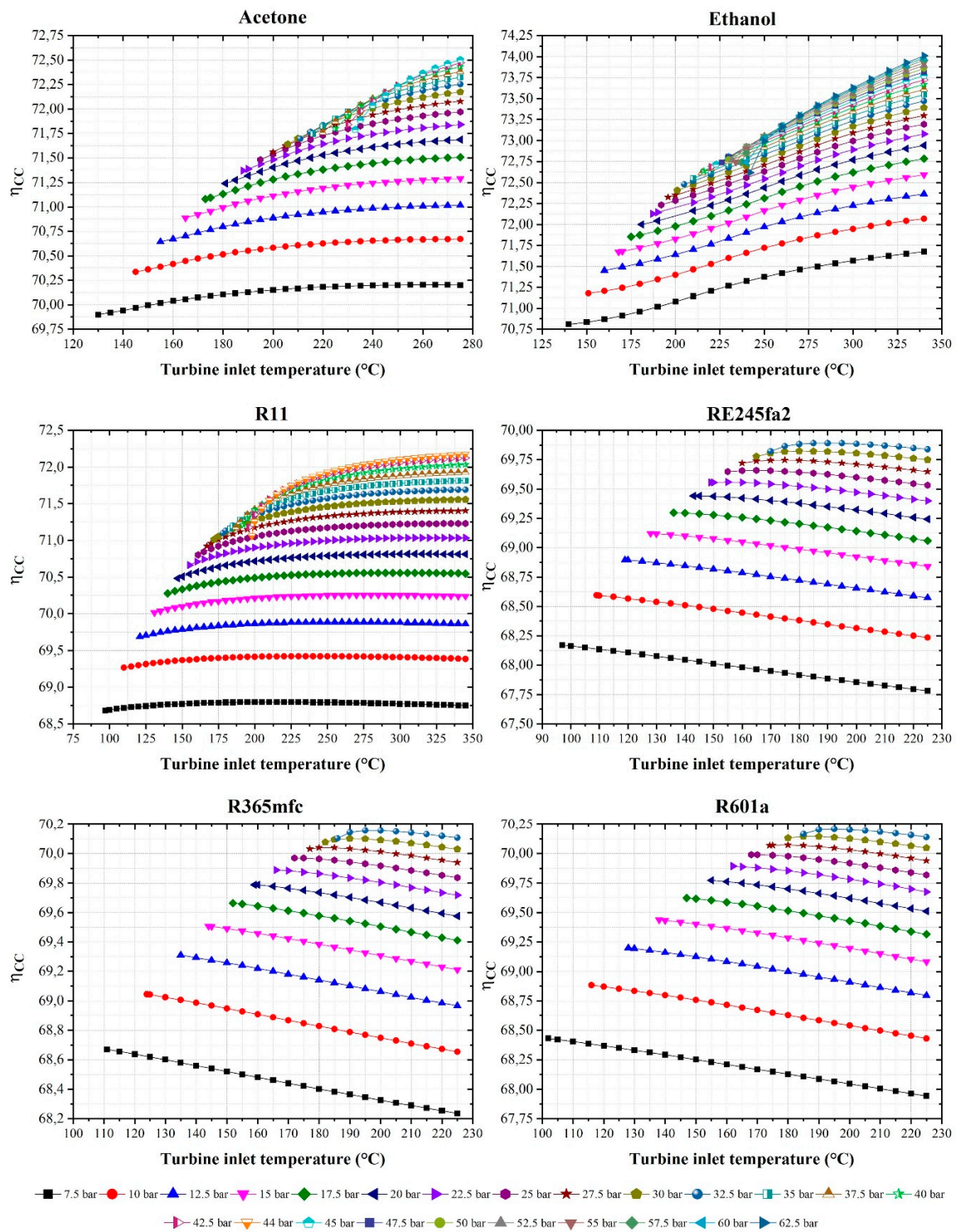


Figure 9. The change in the thermal efficiency of the cogeneration cycle by considering the selected organic working fluids, ORC-turbine inlet temperature and ORC-turbine inlet pressure.

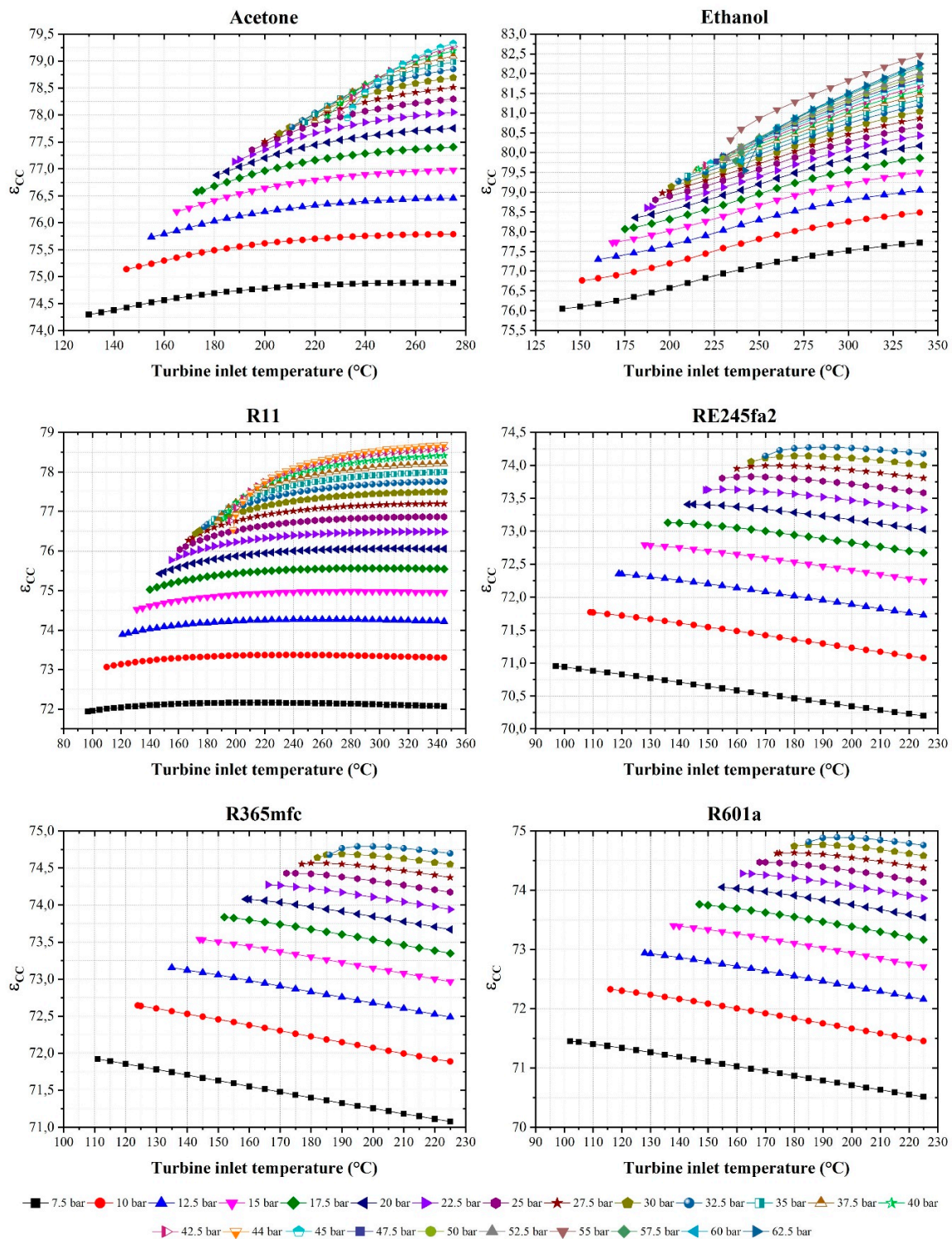


Figure 10. The change in exergy efficiency of the cogeneration cycle by considering the selected organic working fluids, ORC-turbine inlet temperature and ORC-turbine inlet pressure.

6. Conclusions

In the present study, the possibility of the improvement in a present waste chip burning system was analysed for the case of integrating ORC. In the scope of the study, firstly, the ORC was parametrically optimised for six selected different type working fluids (acetone, ethanol, R11, RE245fa2, R365mfc and R601a), with varying turbine inlet temperature and turbine inlet pressure. The turbine inlet

temperature of the ORC was increased from the saturated steam temperature of the fluid to the maximum temperature of the fluid. The turbine inlet pressure of the ORC was increased from 7.5 bar to the critical pressure of the fluid. Moreover, in order to compare the performance of the working fluids, the turbine outlet pressure (condensing pressure) was selected of the saturation pressure of the working fluids at 30 °C. Secondly, by considering the performance data evaluated from parametric optimisation of the ORC, the improvement in the cogeneration cycle was analysed in term of thermal and exergy efficiencies.

As a result of the parametric optimisation of the ORC, different changing trends of the performance parameters of the ORC were observed at a constant turbine inlet pressure, depending on the fluid type. At a constant turbine inlet pressure, the performance parameters of the ORC increased with increasing turbine inlet temperature for wet and isentropic type working fluids (acetone, ethanol and R11). However, for dry type working fluids, two changing trends in the performance parameters of the ORC were observed. At constant turbine inlet pressure, the performance parameters of the ORC were decreased with increasing turbine inlet temperature up to high turbine inlet pressure levels. At high turbine inlet pressure levels, the performance parameters of the ORC were first increased up to a certain turbine inlet temperature and then decreased with increasing turbine inlet temperature.

When comparing the gross thermal efficiency with net thermal efficiency, the effect of the working fluid on the ORC is obviously seen, because the minimum net and gross thermal efficiencies of each working fluid were calculated at the same turbine inlet temperature and turbine pressure. However, the maximum net and gross thermal efficiencies of each working fluid are only found at the same turbine inlet temperature and turbine pressure for the wet and isentropic type working fluids. The maximum net and gross thermal efficiencies dry type working fluids were calculated at the same turbine inlet pressure, but with different turbine inlet temperatures. This is thought to result from the mass flow rate and pump power consumption at high pressure levels.

The maximum performance of the ORC was obtained from the ORC with ethanol, which is a wet type of working fluid. The maximum net power, net thermal efficiency and exergy efficiency were calculated as 453.91 kW, 30.01% and 67.56% at 340 °C and 62.5 bar from the ORC with ethanol, respectively.

When the performance of the overall cogeneration cycle considered in the current system, the exhaust gas is cooled in the heat exchanger to use in the fibre drying process. The released heat in the heat exchanger is thrown directly to the atmosphere without use. With the present study, an alternative cogeneration cycle was suggested by adding ORC to the system. After parametric optimisation and detailed calculations, almost 30% of the wasted heat was calculated as recoverable by use of ORC with ethanol. By using the designed cogeneration system, it was calculated that the thermal efficiency of the system can be increased up to 74.01%.

When the exergy efficiency results of the ORC for varying turbine inlet pressure and turbine inlet temperature considered together, the maximum exergy efficiency of the combined cycle was calculated as 82.24% for ethanol used ORC. This means that a considerable amount (82.24%) of the available energy entering the cogeneration cycle by burning of waste chips was used in the system. Integrating the ORC cycle to the present system will improve the overall performance of the system and reduce the adverse effect on the environment and global warming.

The maximum performance of the cogeneration cycle was obtained by use of the ORC with ethanol. The maximum thermal efficiency and exergy efficiency was calculated as 74.01% and 82.24% for the use of the ORC with ethanol at 340 °C and 62.5 bar, respectively.

The ethanol is flammable and has toxicity. Therefore, the use of ethanol in ORC as a working fluid needs high consideration of the safety and precautions. Therefore, further research is needed, focusing on the precautions to eliminate the adverse effect of these fluids by alternative systems such microelectronic systems (cooling of CPU).

Author Contributions: Y.K. decided the designing condition of the system, system limitations, designed and simulated the system, prepared the graphics, analysed and discussed simulation results in detail and wrote the article. All calculations and writing process of the present manuscript was made by Y.K.

Funding: This research received no external funding.

Conflicts of Interest: The authors declare no conflict of interest.

Nomenclature

\dot{E}	exergy flow (kW)
\dot{Q}	heat flow (kW)
T_0	ambient temperature (°C)
\dot{W}	power (kW)
\dot{m}	mass flow rate (kg/s)
CC	cogeneration cycle
GWP	global warming potential
h	enthalpy (kJ/kg)
ODP	ozone depletion potential
ORC	organic Rankine cycle
P	pressure (bar)
LHV	low heating value
T	temperature (°C)
s	entropy (kJ/kgK)

Greek letters

ψ	specific exergy (kJ/kg)
ε	exergetic efficiency (%)
ϵ	burner effectiveness (%)
η	thermal efficiency (%)

Subscripts

<i>boil</i>	boiling
<i>cond</i>	condensing
<i>crt</i>	critical
<i>d</i>	destruction
<i>e</i>	exit
<i>i</i>	inlet
<i>max</i>	maximum
<i>surr</i>	heat transfer surface
<i>wc</i>	waste wood chips

References

1. Aghbashlo, M.; Tabatabaei, M.; Soltanian, S.; Ghanavati, H.; Dadak, A. Comprehensive exergoeconomic analysis of a municipal solid waste digestion plant equipped with a biogas genset. *Waste Manag.* **2019**, *87*, 485–498. [[CrossRef](#)] [[PubMed](#)]
2. Aghbashlo, M.; Tabatabaei, M.; Soltanian, S.; Ghanavati, H. Biopower and biofertilizer production from organic municipal solid waste: An exergoenvironmental analysis. *Renew. Energy* **2019**, *143*, 64–76.
3. Koc, Y.; Yagli, H.; Ozdes, E.O.; Baltacioglu, E.; Koc, A. Thermodynamic Analysis of Solid Waste and Energy Consumption to Reduce the Effects of an Electric Arc Furnace (EAF) on the Environment. *J. Glob. Warm.* (in press).
4. Koç, A.; Yağlı, H.; Koç, Y.; Uğurlu, İ. Dünyada ve Türkiye’de Enerji Görünümünün Genel Değerlendirilmesi. *Eng. Mach. Mag.* **2018**, *59*, 86–114.
5. Ekmekçi, İ.; Yetisken, Y.; Çamdali, Ü. Mass balance modeling for electric arc furnace and ladle furnace system in steelmaking facility in Turkey. *J. Iron Steel Res. Int.* **2007**, *14*, 1–6.
6. Olmez, G.M.; Dilek, F.B.; Karanfil, T.; Yetis, U. The environmental impacts of iron and steel industry: A life cycle assessment study. *J. Clean. Prod.* **2016**, *130*, 195–201.

7. Rana, A.; Kalla, P.; Csetenyi, L.J. Recycling of dimension limestone industry waste in concrete. *Int. J. Min. Reclam. Environ.* **2017**, *31*, 231–250.
8. Singh, N.; Hui, D.; Singh, R.; Ahuja, I.P.S.; Feo, L.; Fraternali, F. Recycling of plastic solid waste: A state of art review and future applications. *Compos. Part B Eng.* **2017**, *115*, 409–422. [[CrossRef](#)]
9. Li, Y.; Zhao, X.; Li, Y.; Li, X. Waste incineration industry and development policies in China. *Waste Manag.* **2015**, *46*, 234–241.
10. Joshi, O.; Grebner, D.L.; Khanal, P.N. Status of urban wood-waste and their potential use for sustainable bioenergy in Mississippi. *Resour. Conserv. Recycl.* **2015**, *102*, 20–26.
11. Khudyakova, G.I.; Danilova, D.A.; Khasanov, R.R. The use of urban wood waste as an energy resource. In *IOP Conference Series: Earth and Environmental Science*; IOP Publishing: Bristol, UK, 2017; Volume 72, p. 012026.
12. Dahou, T.; Dutournié, P.; Limousy, L.; Bennici, S.; Perea, N. Recovery of Low-Grade Heat (Heat Waste) from a Cogeneration Unit for Woodchips Drying: Energy and Economic Analyses. *Energies* **2019**, *12*, 501.
13. Al-Hamamre, Z.; Saidan, M.; Hararah, M.; Rawajfeh, K.; Alkhasawneh, H.E.; Al-Shannag, M. Wastes and biomass materials as sustainable-renewable energy resources for Jordan. *Renew. Sustain. Energy Rev.* **2017**, *67*, 295–314.
14. Hossain, M.U.; Leu, S.Y.; Poon, C.S. Sustainability analysis of pelletized bio-fuel derived from recycled wood product wastes in Hong Kong. *J. Clean. Prod.* **2016**, *113*, 400–410.
15. Tozlu, A.; Özahi, E.; Abuşoğlu, A. Waste to energy technologies for municipal solid waste management in Gaziantep. *Renew. Sustain. Energy Rev.* **2016**, *54*, 809–815. [[CrossRef](#)]
16. Nunes, L.J.; Godina, R.; Matias, J.C.; Catalão, J.P. Evaluation of the utilization of woodchips as fuel for industrial boilers. *J. Clean. Prod.* **2019**, *223*, 270–277. [[CrossRef](#)]
17. Nunes, L.J.; Godina, R.; Matias, J.C.; Catalão, J.P. Economic and environmental benefits of using textile waste for the production of thermal energy. *J. Clean. Prod.* **2018**, *171*, 1353–1360.
18. Barrier, C.; Ghaffariyan, M.R. *A Short Review of Artificial Wood Drying Practice in France*; Forest Industries Research Center: Maroochydore, Australia, 2018.
19. Yağlı, H. Basit ve rejeneratif organik Rankine çevrimi (ORC) tasarımları kullanılarak biyogaz yakıtlı ısı-güç kombine (CHP) motorunun atık ısısının geri dönüştürülebilirliği, enerji ve ekserji analizi. Ph.D. Thesis, Iskenderun Technical University, Iskenderun, Turkey, 2018.
20. Bademlioglu, A.H.; Yamankaradeniz, R.; Kaynakli, O. Exergy Analysis of the Organic Rankine Cycle Based on the Pinch Point Temperature Difference. *J. Therm. Eng.* **2019**, *5*, 157–165.
21. Koç, Y.; Yağlı, H. Isı-Güç Kombine Sistemlerinde Kullanılan Kalina Çevriminin Enerji ve Ekserji Analizi. *Politeknik Dergisi*. (in press). [[CrossRef](#)]
22. Koç, Y.; Yağlı, H.; Koç, A. Exergy analysis and performance improvement of a subcritical/supercritical organic rankine cycle (ORC) for exhaust gas waste heat recovery in a biogas fuelled combined heat and power (CHP) engine through the use of regeneration. *Energies* **2019**, *12*, 575. [[CrossRef](#)]
23. Yagli, H.; Koc, A.; Karakus, C.; Koc, Y. Comparison of toluene and cyclohexane as a working fluid of an organic Rankine cycle used for reheat furnace waste heat recovery. *Int. J. Exergy* **2016**, *19*, 420–438.
24. Bilgiç, H.H.; Yağlı, H.; Koç, A.; Yapıcı, A. Deneysel bir organik Rankine çevriminde yapay sinir ağları (YSA) yardımıyla güç tahmini. *Selçuk Üniversitesi Mühendislik, Bilim ve Teknoloji Dergisi* **2016**, *4*, 7–17.
25. Noussan, M.; Abdin, G.C.; Poggio, A.; Roberto, R. Biomass-fired CHP and heat storage system simulations in existing district heating systems. *Appl. Thermal Eng.* **2014**, *71*, 729–735. [[CrossRef](#)]
26. Uris, M.; Linares, J.I.; Arenas, E. Feasibility assessment of an Organic Rankine Cycle (ORC) cogeneration plant (CHP/CCHP) fueled by biomass for a district network in mainland Spain. *Energy* **2017**, *133*, 969–985.
27. Safari, F.; Dincer, I. Development and analysis of a novel biomass-based integrated system for multigeneration with hydrogen production. *Int. J. Hydrog. Energy* **2019**, *44*, 3511–3526.
28. Ghasemi, A.; Heidarnejad, P.; Noorpoor, A. A novel solar-biomass based multi-generation energy system including water desalination and liquefaction of natural gas system: Thermodynamic and thermoeconomic optimization. *J. Clean. Prod.* **2018**, *196*, 424–437.
29. Khanmohammadi, S.; Atashkari, K. Modeling and multi-objective optimization of a novel biomass feed polygeneration system integrated with multi effect desalination unit. *Therm. Sci. Eng. Prog.* **2018**, *8*, 269–283. [[CrossRef](#)]

30. Yağlı, H.; Koç, Y.; Koç, A.; Görgülü, A.; Tandiroğlu, A. Parametric optimization and exergetic analysis comparison of subcritical and supercritical organic Rankine cycle (ORC) for biogas fuelled combined heat and power (CHP) engine exhaust gas waste heat. *Energy* **2016**, *111*, 923–932. [[CrossRef](#)]
31. Desideri, A.; Gusev, S.; Van den Broek, M.; Lemort, V.; Quoilin, S. Experimental comparison of organic fluids for low temperature ORC (organic Rankine cycle) systems for waste heat recovery applications. *Energy* **2016**, *97*, 460–469.
32. Dickes, R.; Dumont, O.; Daccord, R.; Quoilin, S.; Lemort, V. Modelling of organic Rankine cycle power systems in off-design conditions: An experimentally-validated comparative study. *Energy* **2017**, *123*, 710–727. [[CrossRef](#)]
33. Peris, B.; Navarro-Esbri, J.; Molés, F.; Mota-Babiloni, A. Experimental study of an ORC (organic Rankine cycle) for low grade waste heat recovery in a ceramic industry. *Energy* **2015**, *85*, 534–542.
34. Yang, S.C.; Hung, T.C.; Feng, Y.Q.; Wu, C.J.; Wong, K.W.; Huang, K.C. Experimental investigation on a 3 kW organic Rankine cycle for low-grade waste heat under different operation parameters. *Appl. Therm. Eng.* **2017**, *113*, 756–764. [[CrossRef](#)]
35. Navarro-Esbri, J.; Molés, F.; Peris, B.; Mota-Babiloni, A.; Kontomaris, K. Experimental study of an Organic Rankine Cycle with HFO-1336mzz-Z as a low global warming potential working fluid for micro-scale low temperature applications. *Energy* **2017**, *133*, 79–89. [[CrossRef](#)]
36. Soroureddin, A.; Mehr, A.S.; Mahmoudi, S.M.S.; Yari, M. Thermodynamic analysis of employing ejector and organic Rankine cycles for GT-MHR waste heat utilization: A comparative study. *Energy Convers. Manag.* **2013**, *67*, 125–137. [[CrossRef](#)]
37. Cao, Y.; Gao, Y.; Zheng, Y.; Dai, Y. Optimum design and thermodynamic analysis of a gas turbine and ORC combined cycle with recuperators. *Energy Convers. Manag.* **2016**, *116*, 32–41. [[CrossRef](#)]
38. Khaljani, M.; Saray, R.K.; Bahlouli, K. Comprehensive analysis of energy, exergy and exergo-economic of cogeneration of heat and power in a combined gas turbine and organic Rankine cycle. *Energy Convers. Manag.* **2015**, *97*, 154–165.
39. Li, P.; Han, Z.; Jia, X.; Mei, Z.; Han, X.; Wang, Z. Analysis and comparison on thermodynamic and economic performances of an organic Rankine cycle with constant and one-dimensional dynamic turbine efficiency. *Energy Convers. Manag.* **2019**, *180*, 665–679.
40. White, M.T.; Sayma, A.I. Simultaneous cycle optimisation and fluid selection for ORC systems accounting for the effect of the operating conditions on turbine efficiency. *Front. Energy Res.* **2019**, *7*, 50.
41. Pezzuolo, A.; Benato, A.; Stoppato, A.; Mirandola, A. The ORC-PD: A versatile tool for fluid selection and Organic Rankine Cycle unit design. *Energy* **2016**, *102*, 605–620. [[CrossRef](#)]
42. Yari, M.; Mehr, A.S.; Zare, V.; Mahmoudi, S.M.S.; Rosen, M.A. Exergoeconomic comparison of TLC (trilateral Rankine cycle), ORC (organic Rankine cycle) and Kalina cycle using a low grade heat source. *Energy* **2015**, *83*, 712–722.
43. Yang, A.; Su, Y.; Chien, I.L.; Jin, S.; Yan, C.; Shen, W. Investigation of an energy-saving double-thermally coupled extractive distillation for separating ternary system benzene/toluene/cyclohexane. *Energy* **2019**, *186*, 115756.
44. Mahlia, T.M.I.; Syaheed, H.; Abas, A.E.; Kusumo, F.; Shamsuddin, A.H.; Ong, H.C.; Bilad, M.R. Organic rankine cycle (ORC) system applications for solar energy: Recent technological advances. *Energies* **2019**, *12*, 2930.
45. Lecompte, S.; Ntavou, E.; Tchanche, B.; Kosmadakis, G.; Pillai, A.; Manolakos, D.; De Paepe, M. Review of experimental research on supercritical and transcritical thermodynamic cycles designed for heat recovery application. *Appl. Sci.* **2019**, *9*, 2571.
46. Invernizzi, C.; Binotti, M.; Bombarda, P.; Di Marcoberardino, G.; Iora, P.; Manzolini, G. Water mixtures as working fluids in organic rankine cycles. *Energies* **2019**, *12*, 2629.
47. Chatzopoulou, M.A.; Simpson, M.; Sapin, P.; Markides, C.N. Off-design optimisation of organic Rankine cycle (ORC) engines with piston expanders for medium-scale combined heat and power applications. *Appl. Energy* **2019**, *238*, 1211–1236.
48. Valencia, G.; Fontalvo, A.; Cárdenas, Y.; Duarte, J.; Isaza, C. Energy and exergy analysis of different exhaust waste heat recovery systems for natural gas engine based on ORC. *Energies* **2019**, *12*, 2378.
49. Yang, J.; Ye, Z.; Yu, B.; Ouyang, H.; Chen, J. Simultaneous experimental comparison of low-GWP refrigerants as drop-in replacements to R245fa for Organic Rankine cycle application: R1234ze (Z), R1233zd (E), and R1336mzz (E). *Energy* **2019**, *173*, 721–731.

50. Song, C.; Gu, M.; Miao, Z.; Liu, C.; Xu, J. Effect of fluid dryness and critical temperature on trans-critical organic Rankine cycle. *Energy* **2019**, *174*, 97–109.
51. Zhi, L.H.; Hu, P.; Chen, L.X.; Zhao, G. Parametric analysis and optimization of transcritical-subcritical dual-loop organic Rankine cycle using zeotropic mixtures for engine waste heat recovery. *Energy Convers. Manag.* **2019**, *195*, 770–787.
52. Wang, D.; Ling, X.; Peng, H. Performance analysis of double organic Rankine cycle for discontinuous low temperature waste heat recovery. *Appl. Therm. Eng.* **2012**, *48*, 63–71. [[CrossRef](#)]
53. Yamada, N.; Mohamad, M.N.A.; Kien, T.T. Study on thermal efficiency of low-to medium-temperature organic Rankine cycles using HFO– 1234yf. *Renew. Energy* **2012**, *41*, 368–375.
54. Wang, E.H.; Zhang, H.G.; Fan, B.Y.; Ouyang, M.G.; Zhao, Y.; Mu, Q.H. Study of working fluid selection of organic Rankine cycle (ORC) for engine waste heat recovery. *Energy* **2011**, *36*, 3406–3418.
55. Chys, M.; van den Broek, M.; Vanslambrouck, B.; De Paepe, M. Potential of zeotropic mixtures as working fluids in organic Rankine cycles. *Energy* **2012**, *44*, 623–632.
56. Marion, M.; Voicu, I.; Tiffonnet, A.L. Study and optimization of a solar subcritical organic Rankine cycle. *Renew. Energy* **2012**, *48*, 100–109.
57. Xi, H.; Li, M.J.; He, Y.L.; Zhang, Y.W. Economical evaluation and optimization of organic Rankine cycle with mixture working fluids using R245fa as flame retardant. *Appl. Therm. Eng.* **2017**, *113*, 1056–1070.
58. Tiwari, D.; Sherwani, A.F.; Kumar, N. Optimization and thermo-economic performance analysis of organic Rankine cycles using mixture working fluids driven by solar energy. *Energy Sources Part A: Recovery Util. Environ. Eff.* **2019**, *41*, 1890–1907.
59. Tchanche, B.F.; Papadakis, G.; Lambrinos, G.; Frangoudakis, A. Fluid selection for a low-temperature solar organic Rankine cycle. *Appl. Therm. Eng.* **2009**, *29*, 2468–2476.
60. David, G.; Michel, F.; Sanchez, L. Waste heat recovery projects using Organic Rankine Cycle technology—Examples of biogas engines and steel mills applications. In Proceedings of the 2011 World Engineers Convention, Geneva, Switzerland, 4–9 September 2011.
61. Gu, Z.; Sato, H. Performance of supercritical cycles for geothermal binary design. *Energy Convers. Manag.* **2002**, *43*, 961–971.
62. Capata, R.; Gagliardi, L. Experimental investigation on the Reynolds dependence of the performance of branched heat exchangers working with organic fluids. *Int. J. Heat Mass Transf.* **2019**, *140*, 129–138.
63. Cengel, Y.A.; Boles, M.A. *Thermodynamics: An Engineering Approach*, 6th ed.; McGraw-Hill Inc.: New York, NY, USA, 2008.
64. Bejan, A.; Tsatsaronis, G.; Moran, M. *Thermal Design and Optimization*; John Wiley: New York, NY, USA, 1996.
65. Dincer, I.; Rosen, M.A. *Exergy: Energy, Environment and SUSTAINABLE Development*, 2nd ed.; Elsevier: Oxford, UK, 2013.
66. Kotas, T.J. *The Exergy Method of Thermal Plant Analysis*; Elsevier: Oxford, UK, 2013.
67. Kahraman, N.; Cengel, Y.A.; Wood, B.; Cerci, Y. Exergy analysis of a combined RO, NF, andEDR desalination plant. *Desalination* **2005**, *171*, 217–232. [[CrossRef](#)]
68. Kahraman, N.; Cengel, Y.A. Exergy analysis of a MSF distillation plant. *Energy Conv. Manag.* **2005**, *46*, 2625–2636.
69. Yağlı, H.; Karakuş, C.; Koç, Y.; Çevik, M.; Uğurlu, İ.; Koç, A. Designing and exergetic analysis of a solar power tower system for Iskenderun region. *Int. J. Exergy* **2019**, *28*, 96–112. [[CrossRef](#)]
70. Koc, Y.; Kose, O.; Yagli, H. Exergy analysis of a natural gas fuelled gas turbine based cogeneration cycle. *Int. J. Exergy* **2019**, *30*, 103–125.
71. Loni, R.; Kasaeian, A.B.; Mahian, O.; Sahin, A.Z. Thermodynamic analysis of an organic rankine cycle using a tubular solar cavity receiver. *Energy Convers. Manag.* **2016**, *127*, 494–503.
72. Dumont, O.; Dickes, R.; De Rosa, M.; Douglas, R.; Lemort, V. Technical and economic optimization of subcritical, wet expansion and transcritical Organic Rankine Cycle (ORC) systems coupled with a biogas power plant. *Energy Convers. Manag.* **2018**, *157*, 294–306.

